Experimental probe of weak-value amplification and geometric phase through the complex zeros of the response function

Mandira Pal,[1] Sudipta Saha,[1] Athira B S,[2] Subhasish Dutta Gupta,[3] and Nirmalya Ghosh[1,2,*]

[1]*Department of Physical Sciences, Indian Institute of Science Education and Research Kolkata, Mohanpur 741246, India*

[2]*Center of Excellence in Space Sciences India, Indian Institute of Science Education and Research Kolkata, Mohanpur 741246, India*

[3]*School of Physics, University of Hyderabad, Hyderabad 500046, India*

(Received 30 November 2018; published 27 March 2019)

We experimentally demonstrate a fundamental relationship between the weak value of an observable and the complex zero of the response function of a system by employing weak measurement on spin Hall shift of a Gaussian light beam. Using this relationship, we show that extremely large weak values far beyond its upper bound in the conventional linear-response regime can be experimentally obtained from the position of the minima of the pointer intensity profile corresponding to the real part of the complex zero of the response function. The imaginary part of the complex zero, on the other hand, is related to the spatial gradient of the geometric phase of light, which in this particular scenario evolves due to the weak interaction and the pre- and postselections of the polarization states. These relationships between the weak value and the complex zeros of the response function may provide new insights on weak measurements in a wide class of physical systems. Extraction of large weak values outside the usual domain of its validity and quantification of small interaction parameters using a physically meaningful and experimentally accessible system property such as the response function may open up a new paradigm of weak measurement.

DOI: 10.1103/PhysRevA.99.032123

I. INTRODUCTION

Weak measurement, after being discovered by Aharonov, Albert, and Vaidman (AAV) [1], remains a rather enigmatic and hotly debated topic in physics [2–7]. A weak measurement process involves weak coupling between the system of interest and a pointer or measurement device. Preselection in a definite initial state and subsequent postselection in a final state which is nearly orthogonal (small parameter ϵ off from the orthogonal state) to the initial state lead to the outcome of the so-called weak value of an observable. Contrary to ideal "strong" measurement, the weak value can lie outside the eigenvalue spectrum of the observable and can also assume complex values. These extraordinary features of weak measurement have attracted much attention in quantum measurements, e.g., for probing quantum paradoxes and for direct measurement of quantum states [8–15]. This concept can be understood using the wave interference phenomena and is therefore equally applicable to interference of quantum matter waves and classical electromagnetic waves. Indeed, the first experimental observation of spin Hall (SH) effect of light was achieved using weak-value amplification [16]. Despite criticisms based on sophisticated statistical analysis on the effectiveness of pre- and postselected (PPS) weak measurements [2–4], the weak-value amplification scheme has proven to be useful in numerous experiments to quantify small physical parameters, enabling its metrological applications in the optical domain and beyond [16–25]. The applications include detection of ultrasensitive beam deflections [16,18,26], high-precision measurements of angular rotation [19], phase shift [22], temporal shift [17,21], frequency shift [20], and so forth. A number of studies have accordingly presented rigorous arguments on the potential benefits of weak-value amplification in realistic experimental situations [5,27–31].

The weak values (A_W) are usually extracted from the shift of the pointer profile, which is conventionally taken to be Gaussian [1,16,32]. However, in AAV's approximation or in the linear-response regime, even though the measurement may remain weak, there is an upper bound of A_W for sufficiently small overlap (corresponding to the minimum of the offset parameter $\epsilon_{\min}$) of the pre- and postselected states [33–35]. Efforts have therefore been delivered to extend the theory of weak PPS measurements beyond the conventional linear-response regime and to provide a more generalized theory by taking into account relevant higher-order terms in the expansion of the coupling parameter and higher-order weak values [30,36–38]. Under certain conditions ensuring sufficiently weak system-pointer coupling, the analytical formula for the pointer deflection has been derived that explicitly involves A_W and holds for its arbitrary large values [36,37]. In this paper, we supplement these efforts by developing and experimentally demonstrating a conceptually interesting yet remarkably simple approach of extracting arbitrarily large weak values across the entire regime of the small parameter ϵ and outside the usual domain of its validity from the complex zero of the response function of the system. Taking an example of the spin Hall shift of a Gaussian light beam [16], we first establish a relationship between the weak value of the polarization observable and the complex zero of the spatial response function of the system. The relationship between the weak value and the real part of the complex zero of the

*Corresponding author: nghosh@iiserkol.ac.in

response function allows one to extract large weak values beyond the conventional limit from the position of the minima of the pointer intensity profile. The imaginary part of the complex zero of the response function, on the other hand, is related to the inverse spatial gradient of the geometric phase of light, the quantification of which also provides direct information on the weak value. The intriguing relationships between the weak values and the complex zeros of the system response function may provide insights and understanding on weak measurements through physically meaningful and experimentally accessible system properties.

II. THEORY

We consider the weak interaction case of spin Hall (or Imbert-Fedorov) shift of a fundamental Gaussian beam due to partial reflection at a dielectric interface. The corresponding polarization operator for the SH shift is defined as [39,40]

$$A^{\mathrm{SH}} = \begin{bmatrix} 0 & i(1+r_p/r_s)\cot\theta_i \\ -i(1+r_s/r_p)\cot\theta_i & 0 \end{bmatrix}. \quad (1)$$

Here, θ_i is the angle of incidence and r_p and r_s are the angle-dependent amplitude reflection coefficients for p (parallel) and s (perpendicular) linear polarizations, respectively. In order to avoid the interplay of the other variant of the beam shift, namely, the Goos-Hänchen (GH) shift in the weak-value amplification, we chose the input or the preselected polarization state to be $|\psi_{\mathrm{in}}\rangle = |\psi_{\mathrm{pre}}\rangle = [1,\ 0]^T$ (p linear polarization), which is the eigenstate of the GH shift [41]. The postselections are done at linear polarization states $|\psi_{\mathrm{post}}\rangle = [\pm\sin(\epsilon),\ \cos(\epsilon)]^T$. Here, ϵ is a small angle by which the postselected state is away from the orthogonal to the input state. The corresponding expression for the weak value of the SH shift can be written as [39]

$$A_W^{\mathrm{SH}} = \frac{\langle\psi_{\mathrm{post}}|A^{\mathrm{SH}}|\psi_{\mathrm{pre}}\rangle}{\langle\psi_{\mathrm{post}}|\psi_{\mathrm{pre}}\rangle} = \pm iR\cot\epsilon, \quad (2)$$

where $R = (1 + r_s/r_p)\cot\theta_i$ [39,42]. Note that the eigenstates of the SH shift are left and right circular (elliptical) polarizations, which yield real eigenvalues corresponding to shift in the coordinate (y) space (spatial shift). Weak-value amplification [Eq. (2)], on the other hand, yields an imaginary weak value representing shift in the conjugate transverse momentum (p_y) space (angular shift). This angular shift is detected as a shift of the centroid (Δy) of the Gaussian beam at the detection plane, which can be related to the weak value as [42]

$$\Delta y = \frac{\lambda}{2\pi}\frac{z}{z_0}\mathrm{Im}\left(A_W^{\mathrm{SH}}\right). \quad (3)$$

Here, λ is the wavelength, z is the propagation distance, z_0 is the Rayleigh range ($z_0 = \frac{\pi w_0^2}{\lambda}$), and w_0 is the beam waist. The above expression for the weak-value amplified shift of the Gaussian beam centroid is bounded by a minimum value of the small offset angle ($\epsilon_{\min} \sim \frac{\delta_p}{w_0}$, where $\delta_p = \frac{\lambda}{2\pi}R$) [16]. Beyond this limit ($\epsilon < \epsilon_{\min}$), extraction of the weak value from the shift of the beam centroid does not follow the prediction of Eq. (2) [33].

In order to establish a connection between the weak value of the polarization observable and the zero of the system response function, we use the generalized expression for the reflected field vector from a dielectric interface for an incident Gaussian beam with linear polarization state $[a_p,\ a_s]^T$ [42]

$$\vec{E}_r \propto \exp\left[k\left(iz - \frac{x^2+y^2}{2(z_0+iz)}\right)\right]\begin{pmatrix} r_p\left(1 - i\frac{x}{z_0+iz}\frac{\partial \ln r_p}{\partial\theta_i}\right) & i\frac{y}{z_0+iz}(r_p+r_s)\cot\theta_i \\ -i\frac{y}{z_0+iz}(r_p+r_s)\cot\theta_i & r_s\left(1 - i\frac{x}{z_0+iz}\frac{\partial \ln r_s}{\partial\theta_i}\right)\end{pmatrix}\begin{pmatrix} a_p \\ a_s\end{pmatrix}. \quad (4)$$

Here, x is the coordinate in the plane of incidence, while y is perpendicular to this plane. As previously noted, here, weak measurement is performed exclusively on transverse (along the y direction) spin Hall shift by nullifying the in-plane (along the x direction) GH shift. Thus, the reflected field amplitude relevant to the weak-value amplification of spin Hall shift for postselection states $\pm\epsilon$ can be obtained by setting $x = 0$ as

$$E_r^W(y) \propto \exp\left[-\frac{ky^2}{2(z_0+iz)}\right] \times G(y),$$
$$G(y) = \left[1 \pm i\frac{y}{z_0+iz}R\cot\varepsilon\right]. \quad (5)$$

The first term can be interpreted as the Gaussian field amplitude of the reflected virtual beam and the second term [G(y)] encodes information on the change in the field distribution due to the weak interaction and postselection. G(y) may thus be treated as the effective spatial response function. Note that this spatial response function for momentum domain spin Hall shift is in precise analogy with the frequency response corresponding to time delay or frequency shifts of Gaussian temporal pulse [43,44]. The root of the response function can be obtained as

$$y_0 = \mp\frac{z - iz_0}{R\cot\varepsilon}, \quad (6a)$$
$$y_0^{\mathrm{real}} = \mp\frac{z}{R\cot\varepsilon} = -\frac{z}{\mathrm{Im}\left(A_{\mathrm{SH}}^w\right)}, \quad (6b)$$
$$y_0^{\mathrm{imag}} = \pm\frac{z_0}{R\cot\varepsilon} = \frac{z_0}{\mathrm{Im}\left(A_{\mathrm{SH}}^w\right)}. \quad (6c)$$

Clearly, for $\epsilon \neq 0$, the root is complex. The weak PPS measurement is performed around this complex zero or in other words postselection at $\pm\epsilon$ moves the zero from the upper to the lower half complex position (y) plane. A complex root also implies that the amplitude (or intensity) of the reflected wave never becomes zero; rather it reaches a finite minimum. The spatial position of this intensity minimum is defined by the real part of the root. As ϵ is reduced to zero, the response function meets a real zero at $y_0 = 0$ and the pointer intensity profile becomes double humped Gaussian.

This is in conformity with the results of previous studies on weak measurements when the PPS measurements are exactly orthogonal [36]. With increasing ϵ within the familiar linear-response regime ($\epsilon > \epsilon_{\min} \sim \frac{\delta_p}{w_0}$), the intensity distribution turns out to be a Gaussian with its centroid shifted by Δy proportional to the weak value ($\propto \cot\epsilon \sim \frac{1}{\epsilon}$ in the limit of small ϵ) as per Eq. (3). However, in the limit $\epsilon < \epsilon_{\min}$, the linear-response results are not applicable and the shape of the pointer distribution changes [33,34]. The real part of the complex zero of the response function [Eq. 6(b)] may then be used in place of the shift of the pointer distribution to extract the weak value. This provides a simple yet unexplored avenue of experimentally extracting arbitrarily large weak values that may lie far beyond its upper bound (corresponding to $\epsilon \ll \epsilon_{\min}$) in the conventional linear-response regime.

The imaginary part of the root is related to the geometric phase of light that evolves during weak measurements. In this particular scenario, the pre- ($|\psi_{\rm pre}\rangle = [1,\ 0]^T$) and postselected states ($|\psi_{\rm post}\rangle = [\pm\sin(\epsilon),\ \cos(\epsilon)]^T$) are homogeneous states. In contrast, the intermediate state following the weak interaction (reflection) is inhomogeneous (space varying) and can be obtained from Eq. (4) as $|\psi_{\rm int}\rangle = [r_p,\ -i\frac{y}{z+z_0}(r_p + r_s)\cot\theta_i]^T$. This sequential evolution of the polarization state leads to the generation of Pancharatnam-Berry (PB) geometric phase ($\Phi_{\rm PB}$) that can be formulated using Pancharatnam's connection [45,46]. In the limit $z \ll z_0$, the corresponding expression becomes

$$\begin{aligned}\Phi_{\rm PB} &= {\rm Arg}(\langle\psi_{\rm post}|\psi_{\rm pre}\rangle\langle\psi_{\rm pre}|\psi_{\rm int}\rangle\langle\psi_{\rm int}|\psi_{\rm post}\rangle)\\ &\approx \pm\frac{yR\cot\epsilon}{z_0},\\ \frac{d\Phi_{\rm PB}}{dy} &= \frac{{\rm Im}\left(A_W^{\rm SH}\right)}{z_0} = \frac{1}{y_0^{\rm imag}}.\end{aligned} \tag{7}$$

The transverse spatial (y) gradient of PB geometric phase leads to a large shift in the transverse momentum (p_y) distribution of the Gaussian beam, manifesting as weak-value amplified momentum domain beam shift [47]. Importantly, Eqs. (6c) and (7) provide an interesting way of quantifying the weak value using interferometric measurement. In what follows, we provide experimental demonstration of the above two concepts.

Note that Eqs. (6) and (7) are derived for the case of weak measurements on momentum domain spin Hall shift of the Gaussian light beam, where the weak value is purely imaginary. Accordingly, the zero of the response function and the spatial gradient of geometric phase are related to the imaginary weak value of the polarization operator. While the exact algebraic expressions connecting these entities depend upon the specific problem, such relationships are universal and may be formulated for a wide class of weak measurement systems with appropriate consideration of the relevant parameter space, observables, choice of the pointer (Gaussian or non-Gaussian), and the general complex nature of weak values [1,19,24,48].

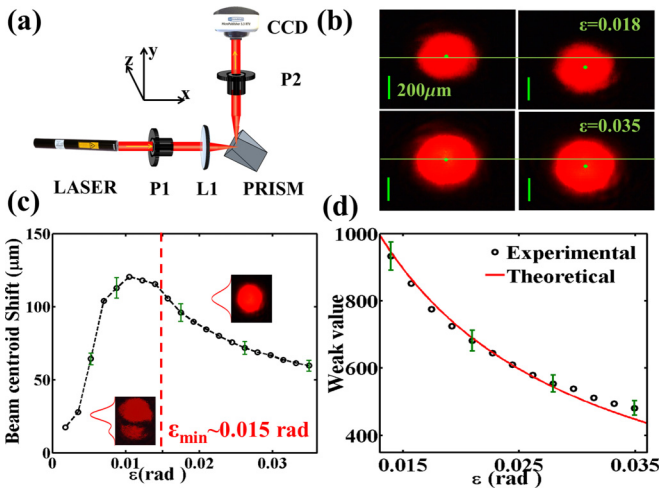

FIG. 1. (a) A schematic of the setup for weak-value amplification of spin Hall shift of a light beam undergoing partial reflection at the air-glass interface. P1 and P2, rotatable linear polarizers; L1, lens. The prism acts as the weak measuring device. (b) Transverse (along y) shift in the beam's centroid between two postselected states $+\epsilon$ (left panel) and $-\epsilon$ (right panel) away from the orthogonal state for the preselected state $|\psi_{\rm pre}\rangle = [1,\ 0]^T$, shown for two values of ϵ : $\epsilon = 0.018$ rad (top panel) and $\epsilon = 0.035$ rad (bottom panel). (c) The shift in the beam's centroid with varying ϵ (open circles). The shape of the reflected beam at two different regimes, ($\epsilon > \epsilon_{\min}$) and ($\epsilon < \epsilon_{\min}$), is displayed. (d) The experimental weak values extracted from the centroid shifts (open circles) and the corresponding theoretical predictions [solid line, Eq. (2)] as a function of varying ϵ within the conventional limit ($\epsilon > 0.015$ rad). The error bars represent standard deviations.

III. RESULTS AND DISCUSSIONS

For probing the real part of the complex zero of the response function, we employed weak PPS measurement on spin Hall shift of the Gaussian light beam undergoing partial reflection at the air-glass interface [Fig. 1(a)]. The fundamental Gaussian mode of the 632.8-nm line of a He-Ne laser was used to seed the system. A rotatable linear polarizer (P1) mounted on a high-precision rotational mount was used to preselect the state at p-linear polarization. The beam was then focused by a lens (L1, focal length = 20 cm) to a spot size of $w_0 = 300\,\mu$m ($z_0 = 45$ cm). The polarization state of light reflected from a $45°-90°-45°$ BK2 prism (refractive index $n = 1.516$) was postselected by another linear polarizer (P2). The exact orthogonal configuration of the pre- and postselected state was located by rotating P2 to obtain the minimum intensity. Postselections were then performed by rotating the polarization axis of P2 to $\pm\ \epsilon$ angle away from this position. The resulting beam shift was detected by a CCD camera (2048×1536 square pixels, pixel dimension $3.45\,\mu$m). The measurements were performed for angle of incidence $\theta_i = 45°$, for a propagation distance $z = 50$ cm ($z > z_0$), and for varying small angle ϵ ($0.0017 < \epsilon < 0.035$ rad).

The minimum value of ϵ corresponding to the upper bound of the weak value in the conventional linear-response regime for the specifics of our experimental parameters is

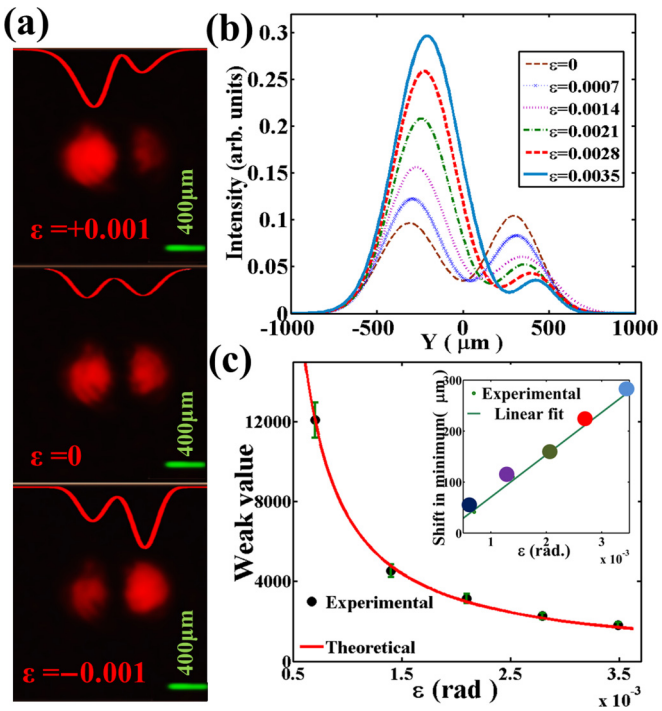

FIG. 2. (a) Observation of intensity minima in the spatial profile of the pointer beam for postselections at $\epsilon < \epsilon_{\min}$ ($\epsilon = \pm\, 0.001$ and 0 rad). (b) Systematic shift of the minima of the pointer intensity profile along the transverse y direction with varying ϵ. (c) The experimental weak values extracted [using Eq. (6b)] from the position of the intensity minimum (solid circles) and the corresponding theoretical predictions (solid line) with varying ϵ. The inset shows the $\sim \epsilon$ scaling of the spatial position of the intensity minimum. The error bars represent standard deviations.

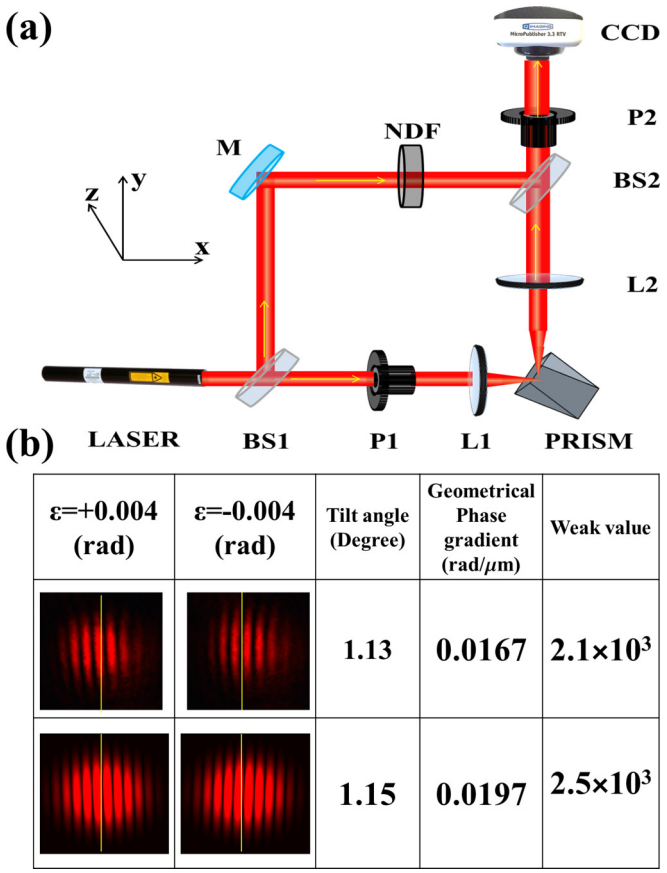

FIG. 3. (a) A schematic of the setup employing weak measurement on spin Hall shift in one arm of a Mach-Zehnder interferometer. P1 and P2, pre- and postselecting linear polarizers, respectively; L1 and L2, lenses; BS1 and BS2, beam splitters; M, mirror; NDF, variable neutral density filter. The experimental parameters are $w_0 = 300\,\mu$m, $z = 5$ cm, and $\theta_i = 45^\circ$. (b) The transverse spatial (y) gradient of geometric phase manifested as opposite tilt of the fringe patterns for typical postselected states at $\pm\epsilon$ (shown for a typical $\epsilon = 0.004$ rad in the top panel). The corresponding theoretical simulations are shown in the bottom panel. The estimates for tilt angle, geometric phase gradient, and weak value $A_W^{\rm SH}$ [using Eq. (7)] are noted.

theoretically estimated using standard Fresnel reflection coefficients of the air-glass interface (for $\theta_i = 45^\circ$) to be $\epsilon_{\min} = \frac{\delta_p}{w_0} \sim 0.015$ rad. Within this limit ($\epsilon > \epsilon_{\min}$), the Gaussian shape of the pointer is retained and systematic transverse shift in the reflected beam's centroid is observed between the postselected states at $\pm\epsilon$ [shown for two different ϵ values in Fig. 1(b), $\epsilon \sim 0.018$ and 0.035 rad]. For values of ϵ below the conventional limit ($\epsilon < 0.015$ rad), the pointer spatial intensity profile deviates from Gaussian shape with the appearance of a pronounced "dip" [inset of Fig. 1(c)]. In this regime, the shift of the beam centroid does not yield the expected weak value with decreasing ϵ [Fig. 1(c)]. For the familiar regime of $\epsilon > 0.015$ rad, on the other hand, the weak values extracted from the centroid shifts [using Eq. (3); see Fig. 1(d)] show reasonable agreement with the corresponding theoretical predictions [Eq. (2)]. Figure 2 demonstrates extraction of large weak values beyond the conventional limit using the real part of the complex zero of the response function. As ϵ is reduced far below this limit, a prominent intensity minimum is observed in the spatial profile of the pointer [Fig. 2(a), shown for $\epsilon = \pm\, 0.001$ rad], which corresponds to the real part of the complex zero of the response function. As ϵ is reduced further to zero, the intensity profile becomes double humped Gaussian, yielding a real zero of the response function at $y_0 = 0$ [Fig. 2(a)]. Systematic shift of the minima of the pointer intensity profile can be observed in this regime of ϵ ($0 < \epsilon < \epsilon_{\min}$) [Fig. 2(b)]. In agreement with Eq. 6(b), the position of the intensity minimum scales as $\sim \frac{1}{\cot\epsilon}$ ($\sim \epsilon$ in the limit of small ϵ) [inset of Fig. 2(c)]. The weak values extracted from the position of the intensity minimum show satisfactory agreement with the corresponding theoretical estimates [Fig. 2(c)]. These results provide conclusive evidence of the relationship between the real part of the complex zero of the response function and the weak value and demonstrate that using this one can quantify small interaction parameters (tiny spin Hall shift here) from weak values that may lie outside the usual domain of its validity.

In order to probe the imaginary part of the complex zero of the response function, we adopted weak PPS measurement on spin Hall shift in one arm of a Mach-Zehnder interferometer [Fig. 3(a)]. Measurements were performed in a similar manner as in Fig. 1(a) ($w_0 = 300\,\mu$m, $z_0 = 45$ cm, $\theta_i = 45^\circ$). However, as apparent from Eq. (7), in order to observe

the PB geometric phase one has to be sufficiently close to the weak interaction plane ($z \ll z_0$). The CCD camera used to record the interference pattern was therefore placed at a distance $z = 5\,\text{cm}$. In agreement with Eq. (7), the transverse spatial (y) gradient of the PB geometric phase is manifested as opposite tilt of the fringe patterns for postselected states at $\pm\epsilon$ [$\epsilon = 0.004$ rad shown in Fig. 3(b) top panel]. The geometric phase gradient extracted from the tilt of the experimental fringe pattern ($0.167\,\text{rad}/\mu\text{m}$) is in agreement with the corresponding estimate for the simulated results ($0.197\,\text{rad}/\mu\text{m}$) using parameters identical to the experimental situation [Fig. 3(b) bottom panel]. The extracted PB phase gradient is subsequently used to determine the weak value of spin Hall shift using Eq. (7). The weak value estimated from the interferometric experiment ($A_W^{\text{SH}} = 2.1 \times 10^3$) agrees well with the corresponding theoretical estimate [using Eq. (2), $A_W^{\text{SH}} = 2.5 \times 10^3$]. Once again the weak value is estimated for the regime of ϵ lying outside the conventional limit ($\epsilon < \epsilon_{\text{min}}$, $\epsilon_{\text{min}} = 0.015$ rad) for the Gaussian pointer. These results establish the relationship between the weak value, geometric phase gradient, and imaginary part of the complex zero of the response function, making it possible to experimentally extract weak values from the geometric phase gradient using interferometric measurements.

IV. SUMMARY

In summary, we have presented experimental demonstration of a fundamental relationship between the weak value of an observable and the complex zero of the response function of a system by employing weak measurement on spin Hall shift of a Gaussian light beam. The relationship between the weak value and the real part of the complex zero of the response function offered a remarkably simple experimental approach of obtaining extremely large weak values beyond its upper bound in the conventional linear-response regime. The imaginary part of the complex zero of the response function is shown to be related to the gradient of the geometric phase that evolves during weak PPS measurements. This also offered an interferometric approach of extracting extremely large weak values through quantification of the geometric phase gradient. Use of the complex zero of the system response function to extract arbitrarily large weak values and to extract small interaction parameters beyond the conventional limit of validity of weak values may open up a new paradigm of weak measurement. The relationship between the weak values and the complex zeros of the response function may also bear fundamentally interesting consequences in the general scenario of weak measurements.

ACKNOWLEDGMENTS

The authors acknowledge the Indian Institute of Science Education and Research, Kolkata for the funding and facilities. M.P. acknowledges Department of Science & Technology, INSPIRE, Govt. of India for research fellowship. A.B.S. is grateful to Ministry of Human Resources Development, Govt. of India, for research fellowship through Center of Excellence in Space Sciences India.

[1] Y. Aharonov, D. Z. Albert, and L. Vaidman, Phys. Rev. Lett. **60**, 1351 (1988).
[2] C. Ferrie and J. Combes, Phys. Rev. Lett. **112**, 040406 (2014).
[3] G. C. Knee, J. Combes, C. Ferrie, and E. M. Gauger, Quantum Meas. Quantum Metrol. **3**, 32 (2016).
[4] C. Ferrie and J. Combes, Phys. Rev. Lett. **113**, 120404 (2014).
[5] G. C. Knee and E. M. Gauger, Phys. Rev. X **4**, 011032 (2014).
[6] O. Oreshkov and T. A. Brun, Phys. Rev. Lett. **95**, 110409 (2005).
[7] A. N. Jordan, J. Martínez-Rincón, and J. C. Howell, Phys. Rev. X **4**, 011031 (2014).
[8] J. Z. Salvail, M. Agnew, A. S. Johnson, E. Bolduc, J. Leach, and R. W. Boyd, Nat. Photonics **7**, 316 (2013).
[9] J. S. Lundeen, B. Sutherland, A. Patel, C. Stewart, and C. Bamber, Nature (London) **474**, 188 (2011).
[10] Y. Aharonov, A. Botero, S. Popescu, B. Reznik, and J. Tollaksen, Phys. Lett. A **301**, 130 (2002).
[11] N. S. Williams and A. N. Jordan, Phys. Rev. Lett. **100**, 026804 (2008).
[12] P. Campagne-Ibarcq, L. Bretheau, E. Flurin, A. Auffèves, F. Mallet, and B. Huard, Phys. Rev. Lett. **112**, 180402 (2014).
[13] A. Romito, Y. Gefen, and Y. M. Blanter, Phys. Rev. Lett. **100**, 056801 (2008).
[14] L. A. Rozema, A. Darabi, D. H. Mahler, A. Hayat, Y. Soudagar, and A. M. Steinberg, Phys. Rev. Lett. **109**, 100404 (2012).
[15] S. Kocsis, B. Braverman, S. Ravets, M. J. Stevens, R. P. Mirin, L. K. Shalm, and A. M. Steinberg, Science **332**, 1170 (2011).
[16] O. Hosten and P. Kwiat, Science **319**, 787 (2008).
[17] N. Brunner and C. Simon, Phys. Rev. Lett. **105**, 010405 (2010).
[18] P. B. Dixon, D. J. Starling, A. N. Jordan, and J. C. Howell, Phys. Rev. Lett. **102**, 173601 (2009).
[19] O. S. Magaña-Loaiza, M. Mirhosseini, B. Rodenburg, and R. W. Boyd, Phys. Rev. Lett. **112**, 200401 (2014).
[20] D. J. Starling, P. B. Dixon, A. N. Jordan, and J. C. Howell, Phys. Rev. A **82**, 063822 (2010).
[21] G. Strübi and C. Bruder, Phys. Rev. Lett. **110**, 083605 (2013).
[22] X.-Y. Xu, Y. Kedem, K. Sun, L. Vaidman, C.-F. Li, and G.-C. Guo, Phys. Rev. Lett. **111**, 033604 (2013).
[23] L. Zhang, A. Datta, and I. A. Walmsley, Phys. Rev. Lett. **114**, 210801 (2015).
[24] O. Zilberberg, A. Romito, and Y. Gefen, Phys. Rev. Lett. **106**, 080405 (2011).
[25] N. Brunner, V. Scarani, M. Wegmüller, M. Legré, and N. Gisin, Phys. Rev. Lett. **93**, 203902 (2004).
[26] G. Puentes, N. Hermosa, and J. P. Torres, Phys. Rev. Lett. **109**, 040401 (2012).
[27] L. Vaidman, Phil. Trans. R. Soc. A **375**, 20160395 (2017).
[28] L. Vaidman, A. Ben-Israel, J. Dziewior, L. Knips, M. Weißl, J. Meinecke, C. Schwemmer, R. Ber, and H. Weinfurter, Phys. Rev. A **96**, 032114 (2017).

[29] J. Martínez-Rincón, W.-T. Liu, G. I. Viza, and J. C. Howell, Phys. Rev. Lett. **116**, 100803 (2016).
[30] J. Dressel, M. Malik, F. M. Miatto, A. N. Jordan, and R. W. Boyd, Rev. Mod. Phys. **86**, 307 (2014).
[31] G. I. Viza, J. Martínez-Rincón, G. B. Alves, A. N. Jordan, and J. C. Howell, Phys. Rev. A **92**, 032127 (2015).
[32] N. W. M. Ritchie, J. G. Story, and R. G. Hulet, Phys. Rev. Lett. **66**, 1107 (1991).
[33] I. M. Duck, P. M. Stevenson, and E. C. G. Sudarshan, Phys. Rev. D **40**, 2112 (1989).
[34] T. Koike and S. Tanaka, Phys. Rev. A **84**, 062106 (2011).
[35] Y. Susa, Y. Shikano, and A. Hosoya, Phys. Rev. A **85**, 052110 (2012).
[36] S. Wu and Y. Li, Phys. Rev. A **83**, 052106 (2011).
[37] A. G. Kofman, S. Ashhab, and F. Nori, Phys. Rep. **520**, 43 (2012).
[38] A. Di Lorenzo, Phys. Rev. A **85**, 032106 (2012).
[39] K. Y. Bliokh and A. Aiello, J. Opt. **15**, 014001 (2013).
[40] J. B. Götte, W. Löffler, and M. R. Dennis, Phys. Rev. Lett. **112**, 233901 (2014).
[41] M. R. Dennis and J. B. Götte, New J. Phys. **14**, 073013 (2012).
[42] A. Aiello and J. Woerdman, Opt. Lett. **33**, 1437 (2008).
[43] M. Asano *et al.*, Nat. Commun. **7**, 13488 (2016).
[44] D. R. Solli, C. F. McCormick, C. Ropers, J. J. Morehead, R. Y. Chiao, and J. M. Hickmann, Phys. Rev. Lett. **91**, 143906 (2003).
[45] J. Samuel and R. Bhandari, Phys. Rev. Lett. **60**, 2339 (1988).
[46] S. Tamate, H. Kobayashi, T. Nakanishi, K. Sugiyama, and M. Kitano, New J. Phys. **11**, 093025 (2009).
[47] K. Y. Bliokh, Y. Gorodetski, V. Kleiner, and E. Hasman, Phys. Rev. Lett. **101**, 030404 (2008).
[48] R. Jozsa, Phys. Rev. A **76**, 044103 (2007).